Edited by Chuan-Yu Wu

Discrete Element Modelling of Particulate Media

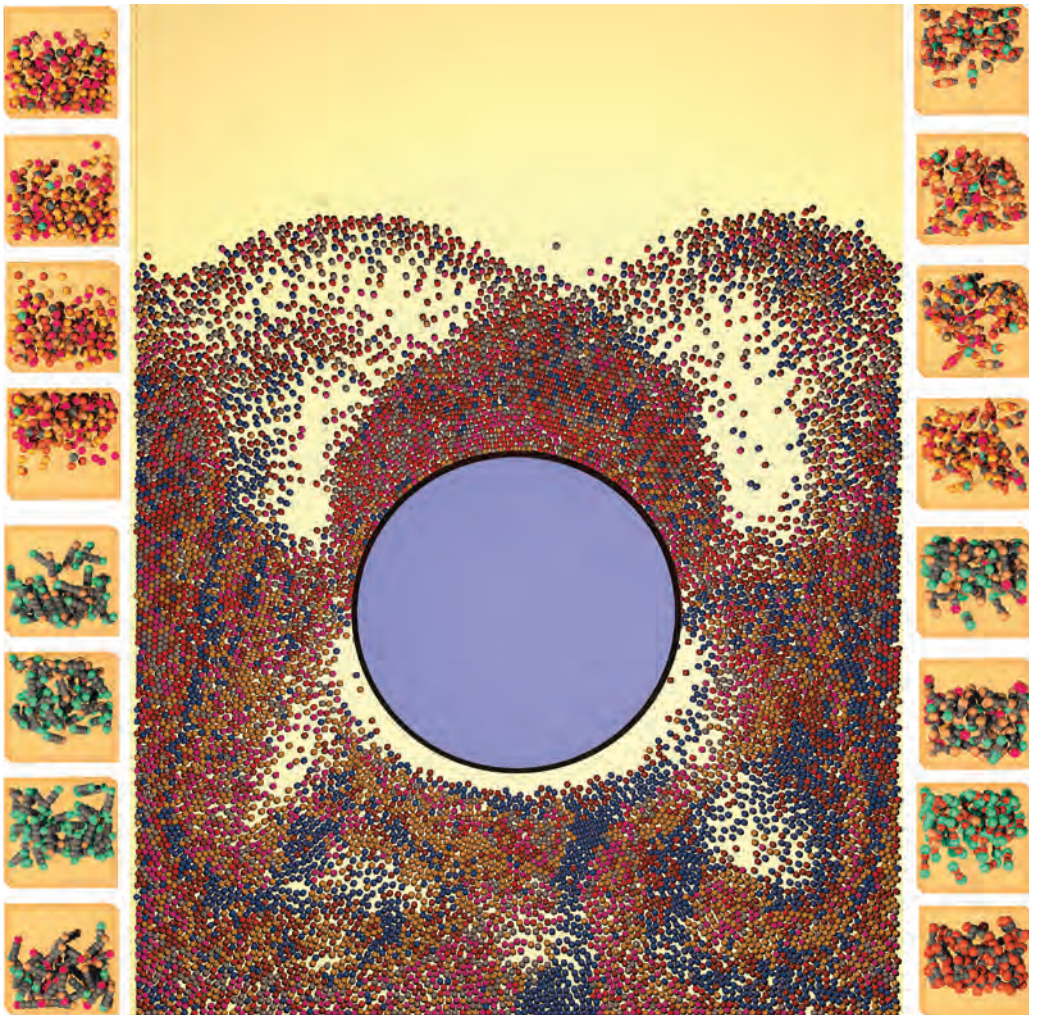

RSC Publishing

Discrete Element Modelling of Particulate Media

Discrete Element Modelling of Particulate Media

Edited by

Chuan-Yu Wu
School of Chemical Engineering, University of Birmingham, Birmingham, UK
Email: C.Y.Wu@bham.ac.uk

RSC Publishing

The proceedings of the International Symposium on Discrete Element Modelling of Particulate Media held at the University of Birmingham on 29-30 March 2012.

Special Publication No. 339

ISBN: 978-1-84973-360-1

A catalogue record for this book is available from the British Library

Published by The Royal Society of Chemistry,
Thomas Graham House, Science Park, Milton Road,
Cambridge CB4 0WF, UK

Registered Charity Number 207890

For further information see our web site at www.rsc.org

Printed in the United Kingdom by CPI Group (UK) Ltd, Croydon, CR0 4YY, UK

PREFACE

The discrete element method (DEM) is a numerical technique for analysing the mechanics and physics of particulate media. It was initially developed to examine the micromechanics of granular media such as sand in the late 1970s and has been significantly advanced ever since. It is now widely employed for modelling of particulate systems across disciplines. As one of the pioneers, Colin Thornton has made enormous contributions to the application of DEM to theoretical soil mechanics and problems in particle technology over the last 25 years or so, especially in the areas of *quasi-static deformation; particle-particle interactions; agglomerate breakage; granular dynamics; liquid bridges and coupled DEM with computational fluid dynamics (CFD).* He has published over 100 papers in this context, including a number of seminal works in the areas of

i) Quasi-static deformation:

- C. Thornton, Numerical simulations of deviatoric shear deformation of granular media, *Geotechnique*, 2000, **50**, 43-53. Times Cited: 169 *(Sources: Web of Science).*
- C. Thornton and S.J. Antony, Quasi-static deformation of particulate media, *Philosophical Transactions of the Royal Society of London Series A-Mathematical Physical and Engineering Sciences*, 1998, **356**, 2763-2782. Times Cited: 94.
- C. Thornton and D.J. Barnes, Computer-simulated deformation of compact granular assemblies, *Acta Mechanica*, 1986, **64**, 45-61. Times Cited: 102.

ii) Particle-particle interaction::

- C. Thornton and Z. Ning, A theoretical model for the stick/bounce behaviour of adhesive, elastic-plastic spheres, *Powder Technology*, 1998, **99**, 154-162. Times Cited: 160.
- C. Thornton and K.K. Yin, Impact of elastic spheres with and without adhesion, *Powder Technology*, 1991, **65**, 153-166. Times Cited: 146.
- C. Thornton, Coefficient of restitution for collinear collisions of elastic perfectly plastic spheres, *Journal of Applied Mechanics-Transactions of The ASME*, 1997, **64** , 383-386. Times Cited: 147.
- C.-Y. Wu, L.Y. Li and C. Thornton, Rebound behaviour of spheres for plastic impacts, *International Journal of Impact Engineering*, 2003, **28**, 929-946. Times Cited: 73.

iii) Liquid bridge:

- G.P. Lian, C. Thornton and M.J. Adams, A theoretical-study of the liquid bridge forces between two rigid spherical bodies. *Journal of Colloid and Interface*, 1993, **161,** 138-147. Times Cited: 212.

iv) Agglomerate breakage

- C. Thornton, Y.Y. Yin and M.J. Adams, Numerical simulation of the impact fracture and fragmentation of agglomerates, *Journal of Physics D-Applied Physics*, 1996, **29**, 424-435. Times Cited: 120.
- G.P. Lian, C. Thornton and M.J. Adams, Discrete particle simulation of agglomerate impact coalescence, *Chemical Engineering Science*, 1998, **53**, 3381-3391. Times Cited: 82.

v) Coupled DEM/CFD

- K.D. Kafui, C. Thornton and M.J. Adams, Discrete particle-continuum fluid modelling of gas-solid fluidised beds, *Chemical Engineering Science*, 2002, **57**, 2395-2410. Times Cited: 109.

Colin Thornton developed leading DEM software for the simulation of quasi-static deformation of dense-phase particulate systems, agglomerate impact coalescence, fracture and attrition, granular flow and gas-solid two phase flow, financially supported by fourteen UK Research Council Grants and eleven industrial contracts. The developed DEM code is so versatile that it not only has the facilities to simulate experiments on three-dimensional polydisperse systems of autoadhesive, elastoplastic spheres, but also incorporates viscous liquid bridges between particles and a 3D Navier-Stokes solver to model the interstitial

fluid. A distinctive feature of the code is that the solid-solid particle interactions are based on theoretical contact mechanics that allow the observed phenomenological behaviour to be related to the experimentally measurable mechanical (elastic, plastic, frictional and adhesive) properties of the constituent particles.

In recognizing the outstanding scientific contributions of Colin Thornton to DEM modelling of particulate media, on the occasion of his 70th birthday, the International Symposium on Discrete Element Modelling of Particulate Media (also known as Thornton Symposium) was held in his honour at the University of Birmingham, UK on 28-30th March, 2012. A total of 92 participants attended the symposium. The symposium programme consisted of 70 contributions (10 keynote presentations, 29 oral presentation and 31 posters), with a wide range of topics including fluidisation, coupled DEM/CFD modelling, particulate flow, quasi-static deformation, cohesive particle systems and liquid-solid systems, fragmentation and electrification. The symposium offered a good opportunity for researchers and scientists to come together to discuss topics pertaining to the modelling of particulate media using DEM and to celebrate Colin Thornton's achievements on this special occasion.

This book contains a collection of papers highlighting the recent advances in discrete element modelling in four areas: i) two-phase systems; ii) cohesive systems; iii) granular flows and iv) quasi-static deformation, inspired by the pioneer work of Colin Thornton. For two-phase systems, recent developments in coupled DEM/CFD are presented, which include drag force models and techniques to enhance the capacity of DEM/CFD to simulate complex flows, including heat and mass transfer. The use of DEM-based coupling methods for modelling liquid-solid systems is discussed. For cohesive systems, the effects of liquid bridges and van der Waals forces on the mechanical behaviour of particle systems, such as lunar soils, wet granular columns and fibre filters, are discussed. For granular flows, the wide application that DEM can offer is showcased, ranging from fundamental granular physics, rock and debris avalanches, excavation of gravels, die filling, silo filling and discharge, and pebble packing in nuclear reactors. For quasi-static deformation, how DEM can be used to explore the micro-mechanics of granular materials is illustrated, especially in simulating triaxial tests and stress wave propagation.

I would like to acknowledge all authors for their efforts and contributions. I also wish to acknowledge the encouragement and guidance of Profs. Jonathan Seville, Mike Adams, Mojtaba Ghadiri and Richard Williams, Drs. Guoping Lian and Ling Zhang, and many others. I am extremely grateful to all members of the organising and scientific committees for their support and advice and the local organising committee for their hard work and dedication in successfully running the symposium.

Finally I thank Colin for his inspiration in discrete element modelling and wish him all the best!

Chuan-Yu Wu
School of Chemical Engineering, University of Birmingham, Birmingham, B15 2TT, UK

May 2012

Contents

Granular Flows

Quasi-Static Deformation

Two-Phase Systems

FROM SINGLE PARTICLE DRAG FORCE TO SEGREGATION IN FLUIDISED BEDS

A. Di Renzo and F. P. Di Maio

Dipartimento di Ingegneria Chimica e dei Materiali, Università della Calabria
Via P. Bucci, Cubo 44A, I-87036 Rende (CS), Italy

1 INTRODUCTION

In numerical simulations of dense two-phase flow involving particulate materials the Discrete Element Method (DEM) has proved particularly effective in capturing the complex hydrodynamics of the solid phase.[1] DEM-based granular solid dynamics, including collisions and persistent contact with elaborate force-displacement laws, friction and cohesion have shown to be superior to traditional fluid-like, continuum approaches, which typically require coarse approximations and the introduction of artificial variables like solids pressure and viscosity. However, computational limitations of DEM models do not allow adding also the burden of flow simulations resolved at the level of particle-particle interstices, so that typically an averaged scale approach, with computational cell sizes of the order of a few particle diameters, is used.[2,3] As a consequence, formulations of the drag force acting on individual particles are required to close the set of equations to solve for the solid and fluid phases. While many drag force models for monodisperse systems have been proposed in the literature, as discussed below, expressions for such force on a particle in a multi-particle system is currently the subject of extensive research work.

2 DRAG FORCE AND CLOSURE IN DEM-CFD MODELS

2.1 Momentum exchange and two-way coupling

Characterisation of the relative motion between a fluid and dense particle system by a DEM-CFD approach requires the solution of the averaged equations of motion of the fluid phase and the classical Newton's second law of dynamics for each particle, where the drag force appears explicitly. The fluid flow field is obtained from the solution of the discretised locally averaged continuity and Navier-Stokes equations, which in differential terms are expressed, respectively, as:

$$\frac{\partial \varepsilon \rho_f}{\partial t} + \nabla \cdot \left(\varepsilon \rho_f \mathbf{U} \right) = 0 \tag{1}$$

$$\frac{\partial(\varepsilon\rho_f \mathbf{U})}{\partial t} + \nabla\cdot(\varepsilon\rho_f \mathbf{U}\mathbf{U}) = -\nabla P + \nabla\cdot\boldsymbol{\tau} + \mathbf{S} + \rho_f \varepsilon \mathbf{g} \tag{2}$$

where ρ_f, $\mathbf{U}$ and P are the fluid density, fluid velocity and pressure, respectively, ε is the volumetric fraction of the fluid (or voidage), $\boldsymbol{\tau}$ is the deviatoric stress tensor, $\mathbf{S}$ is the fluid-particle inter-phase momentum exchange density and $\mathbf{g}$ the acceleration of gravity.

The corresponding equations for each particle of the solid phase follow the conventional DEM approach, i.e.:

$$m\mathbf{a} = m\mathbf{g} + \sum_i \mathbf{f}_{ci} + V\cdot\nabla P + \mathbf{f}_d \tag{3}$$

$$I\boldsymbol{\alpha} = \sum_i (\mathbf{f}_{ci} \times \mathbf{R}_i) \tag{4}$$

where m, V, I, $\mathbf{a}$ and $\boldsymbol{\alpha}$ are the particle mass, volume, moment of inertia, linear and angular acceleration, respectively. The forces considered are gravity, contact forces $\mathbf{f}_c$, pressure gradient and drag force $\mathbf{f}_d$, in the order of appearance in Equation (3). Note that the last two terms arise from the interaction with the fluid. In the rotational direction only torques arising from contact forces are considered.

Interphase coupling is achieved by connecting the momentum exchange density source term $\mathbf{S}$ in Equation (2) with the drag force acting on individual particles, i.e.:

$$\mathbf{S} = \sum_j w_j \mathbf{f}_{dj} \tag{5}$$

where the w_j coefficient plays the role of distance weighting function per unit volume.

2.2 Drag force

Expressions accounting for the influence of velocity and voidage on the drag force exerted on individual particles have been often derived based on established correlations for the pressure drop across fixed beds of a single material of diameter D. In general terms, the modulus of the dissipative pressure gradient is related to the modulus of the drag force by:

$$\nabla p = \frac{1-\varepsilon}{\varepsilon}\frac{6}{\pi}\frac{f_d}{D^3} \tag{6}$$

Extensive studies in the literature led to a number of common, relatively accurate expressions valid for monodisperse suspensions that cover many orders of magnitude of the Reynolds number and from dense packing to highly dilute systems, like the combination of Ergun[3] and Wen and Yu[5] or Di Felice's formula.[6]

In the case of disperse systems or when multiple particulate solids are present simultaneously, the drag force acting on a particle becomes much more difficult to evaluate. This is also related to the fact that experimental accessibility to such datum is very limited. The first theoretical advancements indeed appeared as a result of fully resolved simulations of fluid flow through static arrays of spheres. In particular, van der Hoef et al.,[7] based on lattice-Boltzmann simulations of the flow through random arrays of

spherical particles, were able to propose the first theoretical approach in the characterisation of the phenomenon. The most significant result of their work, later used also in other papers,[8,9] is the formulation of the drag force acting on a generic particle as proportional to the average drag force in the system, and to express the coefficient as a function of a poly-dispersion index and bed voidage, as detailed in the next Section.

3 DRAG IN MULTIPARTICLE TWO-PHASE FLOW

In analogy with the relationship between individual drag force and pressure gradient across the bed, van der Hoef et al.[7] proposed the following starting point:

$$\nabla p = \frac{1-\varepsilon}{\varepsilon}\frac{6}{\pi}\sum_i \frac{x_i f_{di}}{D_i^3} \tag{7}$$

where x_i is the volumetric fraction of species i in the multi-particle mixture. To keep the derivation simple, only two solids will be considered and, without loss of generality, species 1 will be assumed to be the smaller one. The two key steps are (i) the definition of an average drag force $\overline{f_d}$ and average diameter $\overline{D}$ for the system, related to the overall pressure drop by:

$$\nabla p = \frac{1-\varepsilon}{\varepsilon}\frac{6}{\pi}\frac{\overline{f_d}}{\overline{D}^3} \tag{8}$$

and (ii) the definition of the drag force on an individual species as proportional to average drag force in the system, i.e.:

$$f_{di} = \alpha_i \overline{f_d} \tag{9}$$

Then, by introducing the average diameter, as defined by Sauter's mean, and a polydispersion index given, respectively, by:

$$\overline{D} = \left(\frac{x_1}{D_1} + \frac{x_2}{D_2}\right)^{-1} \tag{10}$$

$$y_i = \frac{D_i}{\overline{D}} \tag{11}$$

van der Hoef et al. [7] proposed the proportionality coefficient α_i to be derived based on considerations in the viscous flow regime, giving the individual drag force by:

$$f_{di} = y_i^2 \overline{f_d} \tag{12}$$

It is the case to mention that the derivation presented here is formally different, though conceptually equal, to the original treatment[7] in two aspects. Firstly, a dimensional notation is used here. Secondly, all previous considerations involve the drag force intended

as the net of the pressure gradient interaction term. Additional details can be found in papers elaborating further on the presented approach, e.g. by Cello et al.[10]

4 A MODEL FOR SEGREGATION IN FLUIDISED BEDS

The capability to compute the drag force at the individual particle scale is particularly useful in dealing with fluidised beds of binary mixtures of solids and the related segregation problems. An initially mixed binary bed upon fluidisation shows a tendency for the component with the smaller size and lower density to accumulate to the bed surface, acting as *flotsam*, the reverse occurring for the other component, the *jetsam*. The matter becomes problematic when smaller and denser particles are mixed with larger but less dense particle, a case in which it is difficult even to attribute the roles of flotsam and jetsam to the mixture components.

Despite the severe consequences in process performances, the complexity of the two-phase flow and the substantial previous inability to set the force balance over individual solids species has prevented a theoretical treatment of segregation problems. We have recently proposed[11] to include the result of Equation (12) into a force balance on a particle of, by convention, species 2 immersed in a homogeneous mixture of the two solids.

Under the hypothesis of viscous flow regime, the drag force exerted by the fluid over a particle of diameter D is:

$$f_d = 30\frac{1-\varepsilon}{\varepsilon^2}\pi\mu u D \tag{13}$$

and the corresponding minimum fluidisation velocity is:

$$u_{mf} = \frac{g\varepsilon^3}{180(1-\varepsilon)\mu}\rho D^2 \tag{14}$$

Equations (13) and (14) are intended here applicable to both particle species, provided the appropriate diameter and density are used, as well as the mixture, for which the average size is defined by Equation (10) and the average density is:

$$\bar{\rho} = \rho_1 x_1 + \rho_2(1-x_1) \tag{15}$$

It is useful to recall that the pressure gradient developed as a result of fluidisation of a binary bed is:

$$\nabla p = \bar{\rho}(1-\varepsilon)g \tag{16}$$

The force balance on a particle of species 2 can be set, by comparing the ratio of the hydrodynamic action of the fluid on the particle weight to the value of one, to establish whether it will be pushed upwards or downwards, i.e. it will act as flotsam or jetsam. In formula, this reads:

$$\frac{V_2\overline{\rho}(1-\varepsilon)g + \frac{1}{6}\pi g\varepsilon\overline{\rho}\overline{D}D_2^2}{V_2\rho_2 g} = 1 \tag{17}$$

where the numerator results from the sum of the pressure gradient term (neglecting Archimedean buoyancy) and the drag force evaluated at the minimum fluidisation velocity of the mixture and the denominator is the particle weight. Introducing the dimensionless ratio of the particle-to-average density $\overline{s} = \rho_2/\overline{\rho}$ and of the average-to-particle diameter $\overline{d} = \overline{D}/D_2$, Equation (17) can be rewritten as:

$$\overline{s} = 1 - \varepsilon + \varepsilon\overline{d} \tag{18}$$

Alternatively, using the corresponding version based on the particle-to-particle density and diameter ratios $s = \rho_2/\rho_1$ and $d = D_1/D_2$, we have:

$$s = \frac{x_1}{\dfrac{1}{1-\varepsilon+\varepsilon\left(\dfrac{1}{\frac{x_1}{d}+1-x_1}\right)} - (1-x_1)} \tag{19}$$

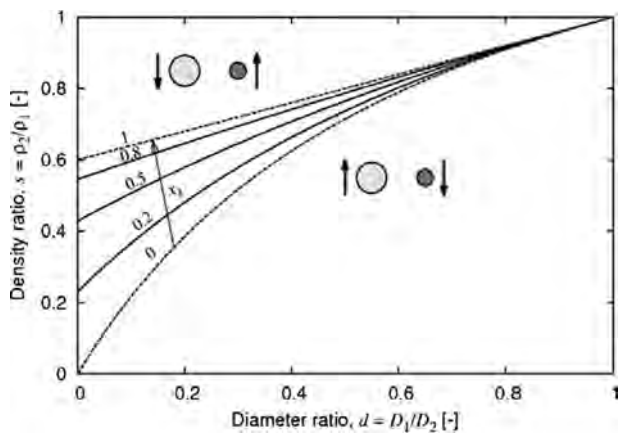

Figure 1 *Equilibrium lines as predicted by Equation (19) with sketches of the segregation direction of the two particle species. The bed voidage equals to 0.4.*

The attention will be focussed on binary mixtures composed of smaller, denser and larger, less dense materials so that values of s and d lie in the range 0 to 1. The possibility for either solid to become the flotsam component determines the occurrence of two possible *segregation directions* of an initially mixed bed. Equilibrium lines that allow discriminating between the two directions can be prescribed by Equation (19) and are shown in Figure 1 at various bed compositions. The chart with the discriminating lines can

be used to predict the tendency for a given solids pair at a given composition to segregate one way or the other. This is achieved by computing s and d to locate the point on the chart and compare its position with the equilibrium line at the corresponding composition.

Similar considerations apply to the comparison of data of a given system in terms of $\bar{s}$ and $\bar{d}$ with the unique equilibrium line prescribed by Equation (18). Comparison of the predicted segregation direction with experimental data available in the literature is shown in Figure 2. Details of the examined systems and further comments are reported elsewhere.[11] However, it is evident that agreement is found for the great majority of the data, without adjustable parameters in the model, confirming the soundness of the approach and, particularly, the realistic predictions of the drag force of Equation (12). Discrete Element simulations are then expected to benefit from the adoption of Equation (12) in modelling fluid-particle flows involving multi-particle mixtures.

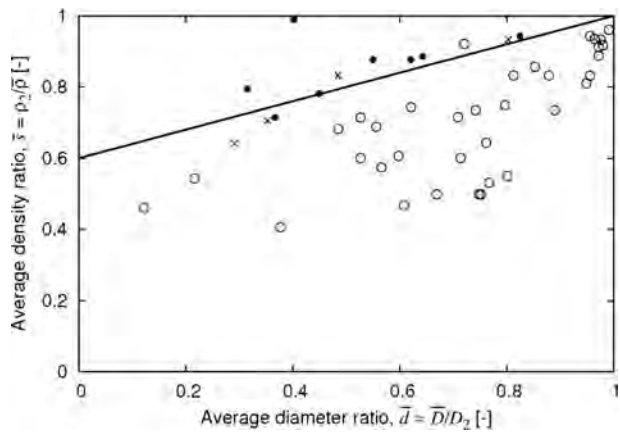

Figure 2 *Experimental data in mixing/segregating systems represented by symbols denoting the flotsam component: open circles for larger but less dense species and solid circles for the smaller and denser species. Crosses represent systems exhibiting bed mixing. The line identifies the equilibrium predicted by Equation (18).*

5 CONCLUSION

Simulations based on Discrete Element Method and averaged CFD approaches require a model for the drag force. In systems involving multi-particle mixtures such drag force is shown to require specific treatment and a recently proposed model is discussed. The same is shown to allow establishing a force balance at the particle scale that proves very useful in addressing problems related to segregation in fluidised beds. Quantitative model validation is shown for a large set of systems available in the literature.

References

1 H.P. Zhu, Z.Y. Zhou, R.Y. Yang and A.B. Yu., *Chem. Eng. Sci.*, 2008, **63**, 5728.
2 K.D. Kafui, C. Thornton and M.J. Adams, *Chem. Eng. Sci.*, 2002, **57**, 2395.

3 M.A. van der Hoef, M. van Sint Annaland, N.G. Deen and J.A.M. Kuipers, *Ann. Rev. Fluid Mech.*, 2008, **40**, 47.
4 S. Ergun, *Chem. Eng. Prog.*, 1952, **48**, 89.
5 C.Y. Wen and Y.H. Yu, *AIChE J.*, 1966, **12**, 610.
6 R. Di Felice, *Int. J. Multiphase Flow,* 1994, **20**, 153.
7 M.A. van der Hoef, R. Beetstra and J.A.M. Kuipers, *J. Fluid Mech.*, 2005, **528**, 233.
8 R. Beetstra, M.A. van Der Hoef and J.A.M. Kuipers, *AIChE J.*, 2007, **53**, 489.
9 S. Sarkar, M.A. van der Hoef and J.A.M. Kuipers, *Chem. Eng. Sci.,* 2009, **64**, 2683.
10 F. Cello, A. Di Renzo and F.P. Di Maio, *Chem. Eng. Sci.*, 2010, **65**, 3128.
11 F.P. Di Maio, A. Di Renzo and V. Vivacqua, *Powder Technol.*, 2012, in press, DOI: 10.1016/j.powtec.2012.04.040.

ENHANCING THE CAPACITY OF DEM/CFD WITH AN IMMERSED BOUNDARY METHOD

C.-Y. Wu[1] and Y. Guo[1,2]

[1]School of Chemical Engineering, University of Birmingham, Birmingham, B15 2TT, UK
[2] Presently with Chemical Engineering Department, University of Florida, Gainesville, FL 32611, USA

1 INTRODUCTION

Discrete Element Methods (DEM) have been coupled with Computational Fluid Dynamics (CFD) for analysing fluid-solid particle flows.[1-4] In the coupled DEM and CFD (*i.e.* DEM/CFD), DEM is used to model the motion of particles and CFD is employed to analyse the fluid flow, while empirical correlations for the drag forces are generally introduced to analyse the interaction between the fluid and particles and two-way coupling of fluid-particle interaction is considered. DEM/CFD is a computationally efficient technique that has been widely used in modelling two-phase flows,[5-8] in which the fluid domain is generally discretised into fluid cells using fixed and rectangular grids and all quantities such as pressure, density and velocity are volume-averaged in the fluid cells. In order to simulate the evolution of bubbles and the detailed fluid flow inside the bubbles, the size of the fluid cell should be smaller than the macroscopic bubbles. On the other hand, it has to be larger than the particle size so that the void fraction (the ratio of the volume of void, excluding that occupied by the solid particles, to the total volume of the cell) will not become zero. Typically, the size of the fluid cell is 3~5 times the particle diameter.[1-3,8]

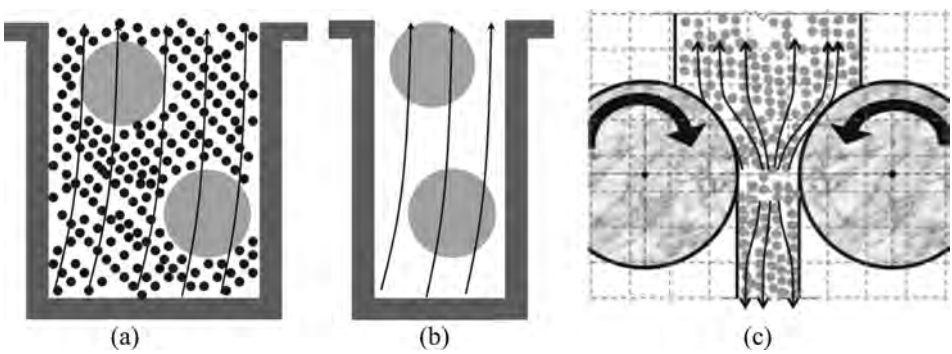

Figure 1 *Illustrations of complex two-phase flows involving (a) particles of significantly different sizes, (b) particles whose sizes are comparable to the fluid domain and (c) moving arbitrary shaped boundaries.*

To some extent, the treatment of fluid domain using large (compare to the size of solids) and regular grids limits the application of DEM/CFD as it is difficult to efficiently model systems with either particles of significantly different sizes (e.g. with particle size ratio higher than 10, see Figure 1a), or particles whose sizes are comparable to the fluid domain (Figure 1b), or moving or arbitrary shaped boundaries that do not conform to the regular grids (Figure 1c). In order to tackle these problems, in this study, an immersed boundary method (IBM), which is used to model the interaction between fluids and large objects or complex boundaries, is incorporated into the DEM/CFD[3] for simulating complex two-phase flows.

2 THE MODIFIED DEM/CFD WITH IBM

For the complex two-phase flow considered, it generally consists of three constituents: i) fine particles; ii) a fluid and iii) large objects and/or complex boundaries (LOCBs), such as moving or arbitrary shaped boundaries. In the modified DEM/CFD with IBM, the motion of each particle is determined using Newton's equations of motion in the DEM. For spherical elastic particles considered in this study, the particle interactions are modelled using the theory of Hertz to determine the normal force,[9] and the theory of Mindlin and Deresiewicz[10] for the tangential force. The classical JKR theory[11-14] is adopted to model the adhesive forces between particles.

The dynamics of the fluid is analysed using CFD, for which the size of the fluid cell is determined by the size of fine particles, not LOCBs (see, *e.g.*, Figure 1c). In other words, the fluid domain is divided into a number of cells of size typically in the range of 3~5 times the particle diameter, irrespective of the presence of LOCBs. The two-way coupling between the fluid and solid particles is modelled using the methods developed by Kafui *et al.*[3] An empirical model proposed by De Felice[15] is used to calculate the drag force on each particle.

To model the interaction between the fluid and LOCBs that are generally much larger than the fluid cells used, an IBM, which was initially proposed to model fluid flows with arbitrary geometrical boundaries,[16] is adopted. In the IBM, an effective void fraction ε in a fluid cell is introduced and defined as the volume fraction of the space not occupied by the fine particles, *i.e.*

$$\varepsilon = 1 - \frac{V_p}{V_c} = \frac{V_{LOCB} + V_f}{V_c} \tag{1}$$

where V_p, V_{LOCB}, V_f and V_c are the volume of the particles, LOCBs, fluid in the cell and the total volume of the cell, respectively. The interfaces between the fluid and LOCBs are assumed to be no-slip and impermeable, and the fluid and LOCBs are treated as a single continuum medium with an unified velocity field $\mathbf{u}$ that is given as

$$\mathbf{u} = \frac{V_f}{V_{LOCB} + V_f}\mathbf{u}_f + \frac{V_{LOCB}}{V_{LOCB} + V_f}\mathbf{U}_{LOCB} \tag{2}$$

where $\mathbf{u}_f$ is the local fluid velocity and $\mathbf{U}_{LOCB}$ is the local solid object velocity or the local velocity of the solid boundary.

The dynamics of the single continuum medium is governed by the following continuity and momentum equations:

$$\frac{\partial\left(\varepsilon_e\rho_f\right)}{\partial t}+\nabla\cdot\left(\varepsilon_e\rho_f\mathbf{u}\right)=0 \tag{3}$$

$$\frac{\partial\left(\varepsilon_e\rho_f\mathbf{u}\right)}{\partial t}+\nabla\cdot\left(\varepsilon_e\rho_f\mathbf{uu}\right)=-\varepsilon_e\nabla p+\varepsilon_e\nabla\cdot\tau-\mathbf{F}_{fp}^{*}+\varepsilon_e\rho_f\mathbf{g}+\tilde{\mathbf{f}} \tag{4}$$

where ρ_f and p are the fluid density and the local fluid pressure, respectively, and t is the time, $\mathbf{g}$ is the gravitational acceleration. The viscous stress tensor, τ, is given as

$$\tau=\left[\left(\mu_b-\frac{2}{3}\mu_s\right)\nabla\cdot\mathbf{u}\right]\delta+\mu_s\left[(\nabla\mathbf{u})+(\nabla\mathbf{u})^T\right] \tag{5}$$

in which μ_b and μ_s are the bulk viscosity and shear viscosity, respectively, and δ is the identity tensor. In Equation (4), the fluid-particle interaction force per unit volume is given as

$$\mathbf{F}_{fp}^{*}=\frac{1}{V_c}\sum_{i=1}^{n_c}\varepsilon\mathbf{f}_{di} \tag{6}$$

in which, n_c is the number of particles in that fluid cell and $\mathbf{f}_{di}$ is the drag force.

In Equation (4), $\tilde{\mathbf{f}}$ is the virtual body force field introduced in the IBM to correct the velocity field at the interfaces between the fluid and LOCBs and inside the LOCBs, so that a desired fluid velocity distribution can be imposed over the solid boundaries. Equation (4) can be discretised using a first order finite difference algorithm as follows

$$\left(\varepsilon_e\rho_f\mathbf{u}\right)^{n+1}=\left(\varepsilon_e\rho_f\mathbf{u}\right)^{n}+\mathbf{H}^{n}\cdot\Delta t-\left(\varepsilon_e\nabla p\right)^{n+1}\cdot\Delta t+\tilde{\mathbf{f}}^{n+1} \tag{7}$$

where

$$\mathbf{H}=-\nabla\cdot\left(\varepsilon_e\rho_f\mathbf{uu}\right)+\varepsilon_e\nabla\cdot\tau-\mathbf{F}_{fp}^{*}+\varepsilon_e\rho_f\mathbf{g} \tag{8}$$

and Δt is the time step and the superscripts, n and $n+1$, indicates the number of time step.

If the entire fluid cell is outside the LOCB, i.e. the volume fraction of the LOCB in the cell $\alpha=V_{LOCB}/V_c=0$. The virtual body force $\tilde{\mathbf{f}}^{n+1}$ can be given as

$$\tilde{\mathbf{f}}^{n+1}=0 \tag{9a}$$

If the fluid cell is inside the LOCB, i.e. $\alpha=1$, then

$$\tilde{\mathbf{f}}^{n+1}=\frac{\left(\varepsilon_e\rho_f\mathbf{U}_{LOCB}\right)^{n+1}-\left(\varepsilon_e\rho_f\mathbf{u}\right)^{n}}{\Delta t}-\mathbf{H}^{n}+\left(\varepsilon_e\nabla p\right)^{n+1} \tag{9b}$$

If the fluid cell is partially occupied by the LOCBs, *i.e.* $0 < \alpha < 1$, we have

$$\tilde{\mathbf{f}}^{n+1} = \alpha \left[\frac{\left(\varepsilon_e \rho_f \mathbf{U}_{LOCB}\right)^{n+1} - \left(\varepsilon_e \rho_f \mathbf{u}\right)^{n}}{\Delta t} - \mathbf{H}^{n} + \left(\varepsilon_e \nabla p\right)^{n+1} \right] \tag{9c}$$

The motion of free moving LOCBs, such as the large particles shown in Figures 1a and 1b, can be obtained by solving the Newton's equations of motion given as

$$\frac{d\left(\tilde{m}\tilde{\mathbf{v}}\right)}{dt} = -\int_{V_T} \tilde{\mathbf{f}} dV + \mathbf{f}_c + \tilde{m}\mathbf{g} \tag{10a}$$

$$\frac{d\left(\tilde{I}\tilde{\boldsymbol{\omega}}\right)}{dt} = -\int_{V_T} \left(\mathbf{r} \times \tilde{\mathbf{f}}\right) dV + \mathbf{T}_c \tag{10b}$$

where $\tilde{m}$, V_T and $\tilde{I}$ are the mass, total volume and the moment of inertia tensor of the LOCB, respectively, $\mathbf{f}_c$ and $\mathbf{T}_c$ are the contact force and the torque exerted by the contacts with particles, $\tilde{\mathbf{v}}$ and $\tilde{\boldsymbol{\omega}}$ are the translational and angular velocities of the LOCB, respectively.

The IBM discussed above is successfully implemented in the DEM/CFD model developed by Kafui *et al.*[3] The details of the numerical implementation are given in Ref. [18]. In this paper, the model verification is presented in the next section and some case studies are given in Section 4 in order to illustrate the robustness and applicability of the modified DEM/CFD with an IBM.

3 MODEL VERIFICATION

In order to verify the modified DEM/CFD, separation of binary mixtures of equal sized bronze/glass beads in a vertically vibrating container in the presence of air, which mimics the physical experiments conducted by Burtally et al.,[19] is simulated in 2D. The model set up is shown in Figure 2a. In this simulation, the IBM is used to model the interaction between air and the moving boundaries (i.e. the walls of the vibrating container) that are assumed to be no-slip and impermeable. The binary mixture consists of 1,250 bronze particles (i.e. the dark-coloured ones) and 3,750 glass particles (the light-coloured ones), which are initially randomly generated and settled in a container of 8.25 × 13.2 mm. All particles have the same diameters of 110 μm. The interparticle and particle-wall friction coefficients are set to 0.3. The materials properties of the particles and the walls are given in Table 1. The air inside the container is assumed to have an initial pressure of 101.325 KPa, density of 1.2 Kg/m^3 and shear viscosity of 1.8X10^{-5} Kg/m.s. The temperature is kept constant at 293 K.

The container is assumed to be a closed system so that the air is enclosed during the whole process. Once all generated particles are settled in the container, it starts to vibrate in a sinusoidal motion with an amplitude of 0.9 mm and a frequency of 55 Hz. The powder patterns during the vibration are shown in Figure 2. It is clear that as the container vibrates, the heavy bronze particles start to congregate and form clusters (Figures 2b & 2c). These clusters gradually merge into a single band (Figures 2d & 2e), which is immersed in between the light glass particles, forming a sandwich structure (Figure 2f). Inside the band,

some light glass particles are entrapped. These features are identical to those observed experimentally by Burtally *et al.*,[19] as shown in Figure 3. This illustrates that the modified DEM/CFD with the IBM is robust and can be used to model two-phase flows with moving boundaries accurately.

Table 1 *Material properties of the particles and the container walls*

Materials	Density (Kg/m^3)	Young's Modulus (GPa)	Poisson's ratio
Bronze particles	8900	110	0.3
Glass particles	2525	63	0.3
Container walls	2525	63	0.3

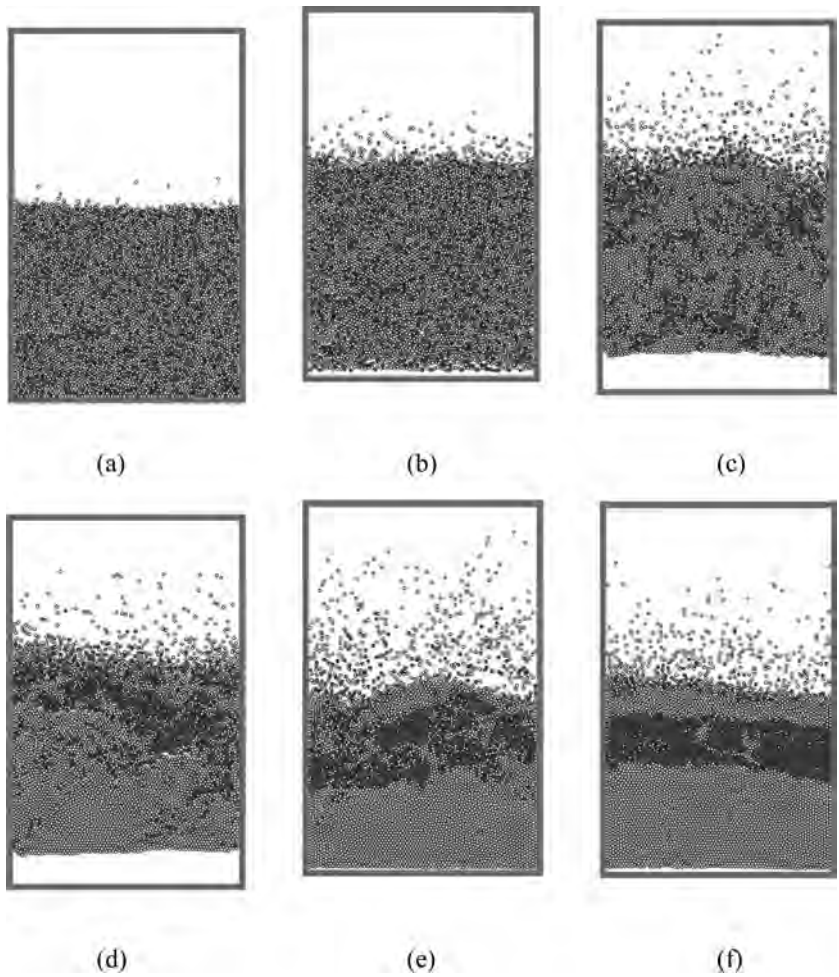

Figure 2 *Separation of a binary mixture under vertical vibration*

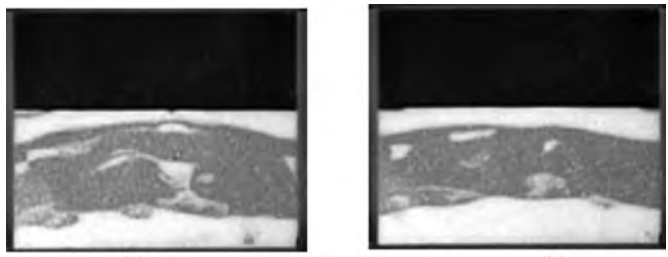

Figure 3 *Separation of a binary mixture and the formation of the sandwich structure during vertical vibration*[19]

4 NUMERICAL EXAMPLES

To further illustrate how the incorporation of the IBM enhances the capacity of the DEM/CFD, two examples of complex two-phase flows involving large objects or moving and circular shaped boundaries are presented here: i) fluidisation with a large inclusion and ii) roll compaction in the presence of air. Although both examples are simulations in 2D, the modified DEM/CFD with an IBM can be readily used to analyse problems in 3D, such as pneumatic conveying in a cylindrical pipe.[18]

4.1 Fluidisation With a Large Inclusion

For some fluidised beds used in industries, large inclusions, such as pipes, rods and disks, are used for various purposes, including process monitoring, heat and mass transfer, and structure enforcement. These inclusions are generally very large compared to the particles used in the fluidisation. It is of practical importance to understand how the presence of these inclusions affects the fluidisation behaviour. Due to the significant size difference between the inclusion and the particles, the conventional DEM/CFD struggles to handle this problem. Although attempts were made to approximate the boundaries using non-smooth stepwise boundaries, this simplification could result in significant errors in the numerical analysis. Furthermore, this approximation is unable to model the large inclusions when they are moving (i.e. moving boundaries). However, this can be easily modelled using the modified DEM/CFD with the IBM that is employed to model the interaction between the large inclusion and the fluid as illustrated in Figures 4 and 5.

Figure 4 shows the numerical model for fluidisation with a large circular inclusion that can be either stationary or moving (not shown here but details can be found in Guo *et al.* [18]). The 2D bed is 12×18 mm and the inclusion has a diameter of 5mm and located in the middle of the bed and 6.5 mm above the bottom of the bed. A monodisperse particle system consisting of 10,000 particles with a diameter of 0.1 mm, density of 2500 Kg/m^3, Young's Modulus of 8.7 GPa and Poisson's ratio of 0.3, is randomly generated in the bed and pluvially deposited to form the initial bed (Figure 4). The inclusion is assumed to be made of steel with a density of 7900 Kg/m^3, Young's Modulus of 210 GPa and Poisson's ratio of 0.29. The particles in the initial bed are color-banded according to their initial positions for visualising the fluidisation behaviour. The air with the same properties as given in Section 3 is introduced from the bottom of the bed with an initial superficial velocity of 50 mm/s. Periodic boundary conditions were assumed at the side boundaries.

The typical fluidisation behaviour is shown in Figure 5 and quantitative analysis is reported elsewhere.[18] It can be seen from Figure 5 that an air film with varying thickness is intermittently formed below the large inclusion and air bubbles form and pass through the gap between the inclusion and side boundaries. It is also clear that there constantly is a cap of defluidised particles sitting on the top of the inclusion, which is consistent with the experimental observations obtained by Glass and Harrison.[20] This cap with defluidised particles can be avoided if the large inclusion is vibrating horizontally, as demonstrated from the simulations with this modified DEM/CFD with an IBM.[18]

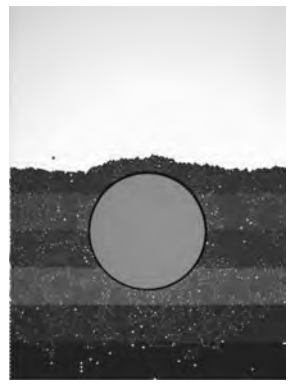

Figure 4 *Initial configuration for fluidisation with a large inclusion*

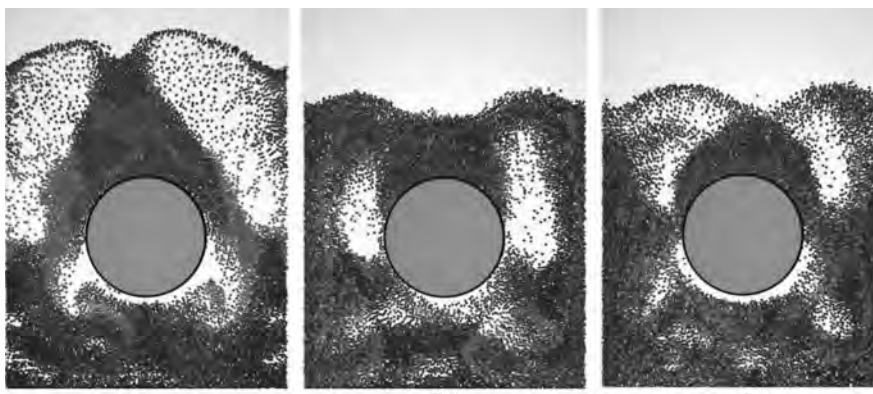

Figure 5 *Typical flow patterns for fluidisation with a stationary large inclusion*

4.2 Roll Compaction in the Presence of Air

Roll compaction is a typical agglomeration process used in pharmaceutical, fine chemicals and other industries to produce granules with increased density and flowability. It uses two counter-rotating rolls to compress dry powders through the narrow roll gap. Powders are roll compacted in the presence of air. Although roll compaction has been investigated intensively over the last two decades, how the presence of air influences roll compaction behaviour of fine powders is still unclear. As the rolls have a circular geometry and move

during the roll compaction process, this cannot be analysed using the conventional DEM/CFD even with stepwise boundaries, but can be modelled using the modified DEM/CFD with IBM presented here, in such a way that the IBM is employed to model the interaction between the rolls and the air. This is illustrated in Figures 6-8.

Figure 6 shows the numerical model for roll compaction in the presence of air, in which 10,000 mono-sized particles are used. The particles have a diameter of 0.1 mm, density of 2500 Kg/m^3, Young's Modulus of 8.7 GPa and Poisson's ratio of 0.3. All friction coefficients are set at 0.3. The rolls are assumed to be steel with a density of 7900 Kg/m^3, Young's Modulus of 210 GPa and Poisson's ratio of 0.3. The particles are initially generated in the fed hopper using the similar approach as discussed in Section 4.1, then discharged from the hopper into the counter rotating rolls. The typical roll compaction behaviour for cohesionless and cohesive powders is presented in Figures 7 & 8, respectively. For the cohesive powder, a surface energy of 1.09×10^{-3} J/m^2 is used. It can be seen that for the cohesionless powder, it can flow easily through the hopper orifice and the roll gap. The powder initially accumulates in the compaction zone between two rolls as the throughput of roll compaction considered here is lower than the mass flow rate from the feed hopper (Figure 7a), while there is less material accumulation in the compaction zone when the cohesive powder is used, but arching/bridging in the hopper and between the two rolls are evident (Figure 8). It is also interesting to note that, as expected, a much higher angle of repose is obtained for the cohesive powder (Figure 8b) compared to the cohesionless powder (Figure 7b). The downflowing powder stream induces a circulation of air current, which could drag fine particles away when fine and light particles are used (Figures 7 & 8).

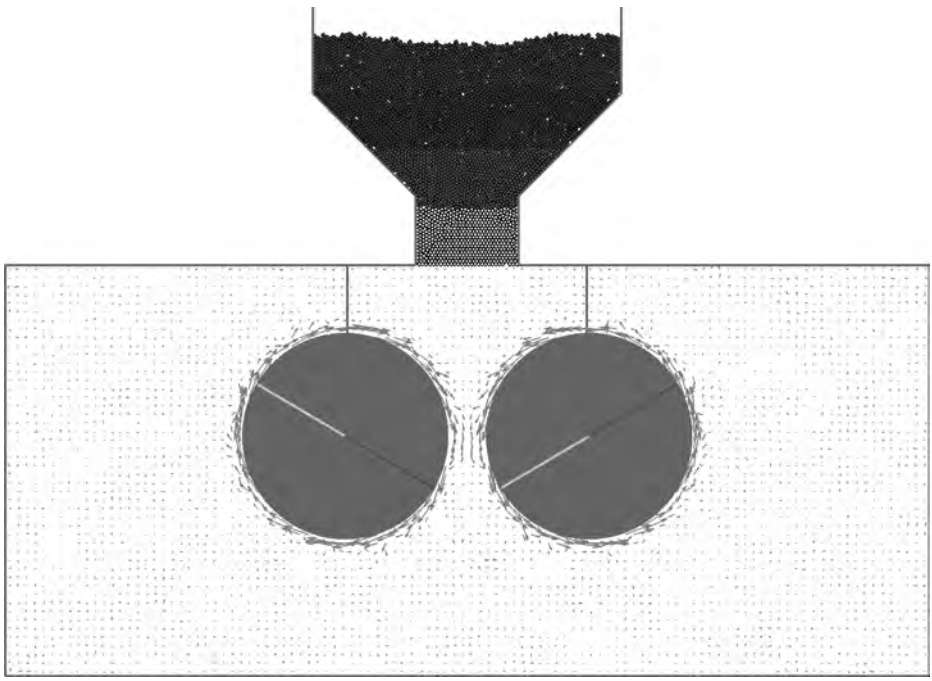

Figure 6 *Initial configuration for roll compaction in the presence of air*

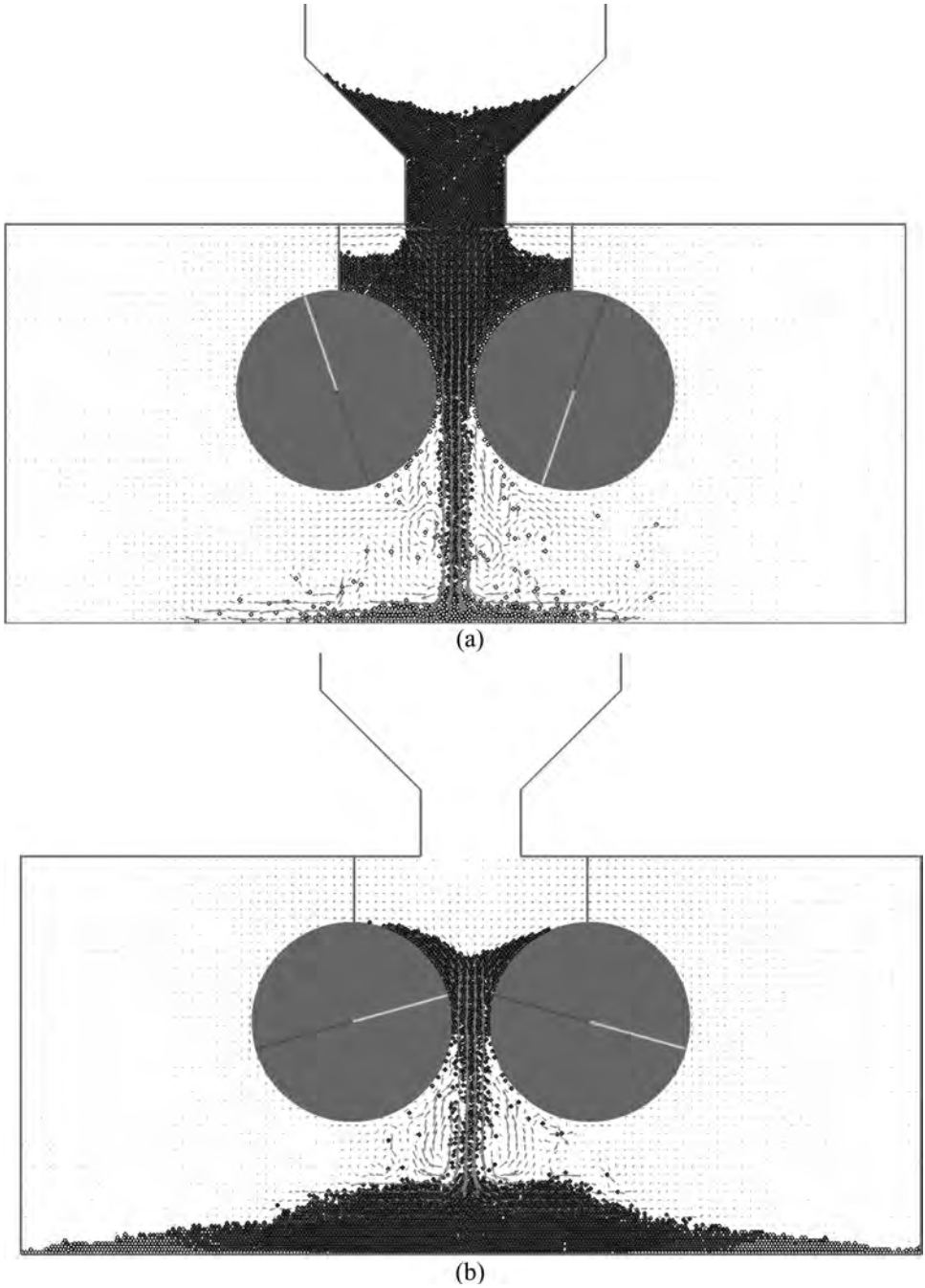

Figure 7 *Typical flow patterns of cohesionless powders during roll compaction in the presence of air*